A Pilot Protection Scheme for HVDC Transmission Lines Based on Simultaneous Existence of Forward and Backward Voltage Travelling Waves

Marvasti, F. Dehghan; Mirzaei, A.; Savaghebi, M.; Jannesar, M. R.

Published in:
Proceedings of 2022 IEEE 13th International Symposium on Power Electronics for Distributed Generation Systems (PEDG)

Link to article, DOI:
10.1109/PEDG54999.2022.9923151

Publication date:
2022

Document Version
Peer reviewed version

A Pilot Protection Scheme for HVDC Transmission Lines Based on Simultaneous Existence of Forward and Backward Voltage Travelling Waves

F. Dehghan Marvasti
Department of Electrical Engineering
Yazd University
Yazd, Iran
farzad_dehghan@stu.yazd.ac.ir

A. Mirzaei
Department of Electrical Engineering
Yazd University
Yazd, Iran
mirzaei@yazd.ac.ir

M. Savaghebi
Department of Engineering Technology
Technical University of Denmark
DK-2750 Ballerup, Denmark
medi@dtu.dk

M. R. Jannesar
Department of Electrical Engineering,
Technical and Vocational University (TVU)
Tehran, Iran
mjannesar@tvu.ac.ir

***Abstract*— A pilot protection method that uses the forward and backward voltage travelling waves to identify DC line faults is proposed in this paper. This method is based on the idea that under internal faults forward and backward travelling waves are observed at both sides of the line within a specific time period. However, under external faults and depending on their direction, backward voltage travelling wave is not observed at one of the terminals. Therefore, a transient-based criterion based on simultaneous existence of line-mode forward and backward voltage travelling waves is proposed. It is shown that the proposed protection method is able to identify internal faults at any location along the line with fault resistance up to 1000 Ω with fast response and high sensitivity and selectivity. Performance evaluations of the proposed protection method is performed using a bipolar MMC-HVDC transmission line, simulated in PSCAD/EMTDC.**

***Index terms*— Forward and backward travelling waves, HVDC protection, pilot protection, travelling wave protection.**

I. Introduction

Large-scale long-distance integration of offshore wind power has become an increasing trend for harvesting electrical energy from wind power resources to meet the economic-benefit goals of clean energy generation [1-2]. Modular multilevel converter-based high voltage direct current (MMC-HVDC) transmission lines are widely used for this purpose for their distinct advantages such as independent active and reactive power control, fast controllability, black start, small footprint and ability to reverse power with low difficulty [3-5]. Despite the valuable advantages, MMC-HVDC systems have low fault-ride-through capabilities as the excessive fault currents can easily damage the power electronic devices inside the converters [6-7]. Therefore, it is of significant importance to devise fast and reliable protection schemes to ensure safe HVDC system operation.

Currently, the majority of HVDC protection schemes consist of travelling wave-based solutions, voltage derivative protection and the traditional current differential scheme [7-8]. Travelling wave-based and voltage derivative methods are of fast response, despite the reliability issues under high-resistance faults [9-10]. To remedy this, current differential protection is utilized, which has superior selectivity in identifying high-resistance faults [11-12]. However, sensitivity to distributed capacitance of the transmission line and slow operation are major vulnerabilities of these methods [13].

Recently, some scholars proposed a number of more robust pilot protection principles. Pilot protection uses a communication link and double-ended measurements to enhance the sensitivity and selectivity in fault detection [11]. There are some novel pilot protection schemes based on under-fault transient energy ratio of DC filters [14], specific frequency current of DC filters [15] and behavior of characteristic harmonic impedances [16]. However, these schemes are more suitable for line commutated converter (LCC) HVDC transmission lines.

Various forms of protective principles based on the application of forward and backward travelling waves are employed in some studies. For example, pilot protection methods based on similarity measure of the voltage travelling waves are proposed in [17-18]. Comparison of the calculated backward voltage travelling wave with that measured at the relay point is used as a fault detection criterion in [19]. In [20], the moments at which the forward and backward travelling wave heads appear at both system terminals are extracted and used for fault discrimination. In [21], amplitude of fault-generated backward travelling waves, obtained from integration of the waves, is used to detect internal faults.

The main objective in this paper is to propose a faster backup protection scheme with lower computational burden and higher sensitivity. The proposed method acts based on the existence of both forward and backward voltage travelling waves under internal faults within a specific time period, which is not observed under external faults. By implementing this idea via using a simple transient-based criterion, the proposed protection method is able to detect internal faults up to 1000Ω with superior response time. The validity of the proposed protection method will be verified using a bipolar MMC-HVDC transmission line simulated in PSCAD-EMTDC.

II. Theory of Travelling Waves

A. HVDC Test System

The schematic diagram of the bipolar HVDC test system and its parameters are presented in Fig. 1 and Table 1, respectively. The bipolar HVDC system transfers power via a 300-km overhead transmission line, which is simulated by the

frequency-dependent line model. The system is also equipped with DC circuit breakers (DCCB) and current limiting inductors (CLI). Four sets of measurement units and protective relays are installed at the sending (S_p, S_n) and receiving (R_p, R_n) terminals of the system. Various fault scenarios ($f_1 - f_7$), consisted of positive-pole-to-ground (PTG), negative-pole-to-ground (NPG) and pole-to-pole (PTP) faults, are also considered for the performance analysis of the proposed protection method.

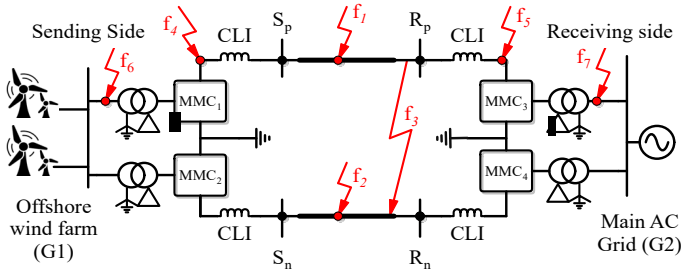

Fig. 1. Schematic diagram of the bipolar MMC-HVDC test system

TABLE I HVDC Test System Specifications

System parameters	Values
AC line voltages of grid side (G1/G2) (rms)	420/400 kV
AC line voltage of valve side (rms)	300kV
Rated DC voltage (pole to ground) (V_{dc})	±500 kV
Rated DC current (I_{dc})	1950A
Rated capacity of converters	1100MVA
Total rated transferred power	2×950MW
CLI	150mH
Converter arm inductor	50mH
Number of submodules per arm	200
Submodule capacitance	8800 μF

B. Initial Voltage Travelling-waves under Fault Scenarios

Travelling wave-based methods are widely used in protective purposes for their fast and accurate response. To understand the application of these methods in protective solutions, the equivalent superposition network of the under-fault HVDC system and the resulted travelling waves should be analyzed carefully. The superposition network can be constructed by adding an extra voltage source at the fault position as the fault incentive source. When DC system faults happen, whether internal or external, forward voltage travelling waves (FVTW) and backward voltage travelling waves (BVTW) are generated from the additional fault voltage source, which propagate along the line in both directions. Travelling wave reflections and refractions occur at discontinuity points for example, at the fault point and the transmission line boundaries. To improve the effectiveness in analyzing these reflections and refractions, the electrical quantities of the system should be decupled first. Therefore, after decoupling the voltage and current quantities, the line-mode forward voltage travelling wave (LFVTW) and the line-mode backward voltage travelling wave (LBVTW) can be calculated by F_1 and B_1 as expressed in (1) and (2) respectively [15].

$$F_1 = (\Delta u_1 + Z_{c1}.\Delta i_1)/2 \quad (1)$$

$$B_1 = (\Delta u_1 - Z_{c1}.\Delta i_1)/2 \quad (2)$$

where Δ_{u1}, Δ_{i1} and Z_{c1} are the line-mode voltage fault component, line-mode current fault component and wave impedance of the transmission line respectively. The positive direction for F_1 is considered from the DC terminals to transmission line, and the positive direction for B_1 is from transmission line to DC terminals. Since the ground-mode voltage components are theoretically zero under pole-to-pole faults, and the attenuation of line-mode travelling waves are lower than those of the ground-mode components, the line-mode voltage traveling waves are the main focus of the analysis in this paper.

According to Fig. 2, when internal fault happens, the fault generated voltage travelling waves propagate along the line until they hit the line boundaries. At these points, the travelling waves are partially reflected to the system and partially refracted to the system beyond the line boundaries. Therefore, multiple reflections and refractions are observed at the line boundaries. The measured quantities of the line-mode voltages at the sending (v_{s1}) and the receiving (v_{r1}) terminals are the summation of the entire forward and backward travelling waves, which can be expressed as follows.

$$\begin{cases} v_{s1} = B_{M1} + F_{M1} + B_{M2} + F_{M2} + \ldots \\ v_{r1} = B_{N1} + F_{N1} + B_{N2} + F_{N2} + \ldots \end{cases} \quad (3)$$

where letters F and B refer to the forward and backward voltage travelling waves and indices with S and R refer to the sending and receiving terminals respectively.

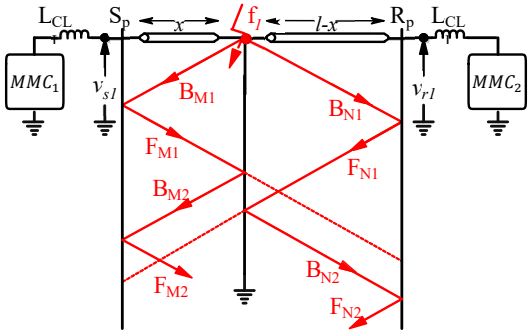

Fig. 2. Travelling wave propagation under internal faults

Similar behavior is observed under external faults. As shown in Fig. 3, for an external fault behind terminal S, multiple reflections and refractions occur. Therefore, similar to (3), the measured voltages at the DC terminals of the line can be obtained as follows.

$$\begin{cases} v'_{s1} = F'_{M1} + B'_{M2} + F'_{M2} + \ldots \\ v'_{r1} = B'_{N1} + F'_{N1} + B'_{N2} + F'_{N2} + \ldots \end{cases} \quad (4)$$

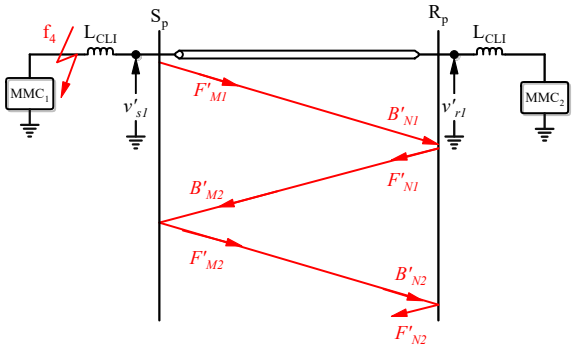

Fig. 3. Travelling wave propagation under external faults

where the definitions of the components of v'_{s1} and v'_{r1} are like those of v_{s1} and v_{r1} in (3).

By comparing Fig. 2 and Fig. 3, it can be seen that under both internal and external faults, multiple reflections and refractions are observed. However, in contrast to the internal fault case, the reflections and refractions under external fault are only happening at the line boundaries, as there is no fault point on the line. By focusing on the initial reflections at each scenario, a distinguishing behavior can be derived. Considering the initial voltage travelling waves, (3) and (4) can be rewritten as (5) and (6) under internal and external faults respectively.

$$\begin{cases} v_{s1} = B_{M1} + F_{M1} \\ v_{r1} = B_{N1} + F_{N1} \end{cases} \tag{5}$$

$$\begin{cases} v'_{s1} = F'_{M1} \\ v'_{r1} = B'_{N1} + F'_{N1} \end{cases} \tag{6}$$

By comparing (5) with (6), it can be seen that during the initial period of the internal faults, totally four forward and backward travelling waves are observed at both DC terminals. However, during the initial period of the external faults, there are 3 forward and backward travelling waves collectively, as the backward travelling wave, B'_{M1}, does not exist. Similarly, for an external fault behind terminal R, the backward travelling wave, B'_{N1}, is missing during the first reflections. Therefore, simultaneous existence of both initial LFVTW and LBVTW at each DC terminal can be used to distinguish internal faults from the external faults, which is the core idea in the design of the proposed pilot protection method.

The proposed fault detection criterion is defined as the rate of change of voltage (ROCOV) applied on the initial LFVTWs and LBVTWs of both terminals. When the fault detection criterion at each terminal discovers the forward and backward travelling waves within a specific time period, the internal fault is confirmed. Otherwise, the situation can be an external fault or any other non-fault disturbances. The realization of this idea and the proposed protection algorithm and its components will be thoroughly discussed in the following section.

III. Proposed Protection Method

The proposed pilot protection method and its components, consisting of the main protection unit and fault pole identification unit, are discussed in this section.

A. Main Protection Unit

In order to lower the computational burden of the main protection unit, a start-up unit is considered in this study to discriminate between faults and normal operation. Due to its robust performance, an undervoltage criterion is considered for the start-up unit as expressed by (7).

$$\Delta v_{sp} < -V_{th\_s} \,||\, \Delta v_{sn} > V_{th\_s} \tag{7}$$

where Δv_{sp} and Δv_{sn} are the DC voltages gradients of the positive and negative poles at the sending terminal respectively. V_{set_s} is the corresponding threshold, which is considered 450 kV. The first sampling point at which the start-up unit is satisfied is denoted by n_s. A very similar starting unit is also utilized at the receiving terminal.

As discussed in section II, rate of change of LFVTW and LBVTW at each terminal is considered as the fault detection criterion. Therefore, a suitable realization of this criterion can be expressed as follows.

$$\begin{cases} C_f = \dfrac{1}{n_t}\sum_{n=n_s}^{n_s+n_t-1}\{v_{s1\_f}(n)\} - \dfrac{1}{n_t}\sum_{n=n_s-5}^{n_s-1}\{v_{s1\_f}(n)\} \\ C_b = \dfrac{1}{n_t}\sum_{n=n_s}^{n_s+n_t-1}\{v_{s1\_b}(n)\} - \dfrac{1}{n_t}\sum_{n=n_s-5}^{n_s-1}\{v_{s1\_b}(n)\} \end{cases} \tag{8}$$

$$C_f < -V_{set\_f} \;\&\; C_b < -V_{set\_b} \tag{9}$$

where V_{s1_f} and V_{s1_b} are the LFVTW and LBVTW at the sending terminal respectively, and V_{set_f} and V_{set_b} are the corresponding setting thresholds. n_t is the number of samples in the data window. The fault detection criterion calculates the median of v_{s1_f} and v_{s1_b} over n_t samples and measures the difference between each value and its corresponding steady-state median quantity over the 5 data samples before n_s. If the difference satisfies (9), an activation signal, as an indication of forward fault, is generated. However, if the fault is external, (9) will not be satisfied. Therefore, (10) is checked to identify the direction of the external fault.

$$C_f < -V_{set\_f} \;\&\; C_b > -V_{set\_b} \tag{10}$$

If (10) is satisfied, a reverse external fault such as f_4 in Fig. 1 is confirmed and consequently, a prevention signal, as an indication of backward external fault, will be generated. The quantity of V_{set_f} and V_{set_b} should be determined in such way that high resistance internal faults can be reliably detected. Therefore, based on the results of C_f and C_b, obtained from a remote-end 1500-Ω internal fault, V_{set_f} and V_{set_b} are considered 25kV. In a very similar way, a protective criterion can be defined for the receiving terminal of the system. Note that, as DC line faults happen, it is expected to see voltage drop along the transmission lines, hence, C_f and C_b, calculated from (8), should have negative values under DC faults.

B. Fault Pole Identification Unit

Since bipolar HVDC systems can be operated in monopolar configuration, it is essential to identify the faulty pole. As thoroughly discussed in [22], the ground-mode voltage component under PTG, PTP and NTG faults, are negative, zero and positive, respectively. Therefore, a criterion for fault pole identification employing the ground-mode forward voltage travelling wave (GFVTW) is defined as (11) and (12) for terminal S.

$$C_p = \frac{1}{n_t}\sum_{n=n_s}^{n_s+n_t-1}\{v_{s0\_p}(n)\} - \frac{1}{n_t}\sum_{n=n_s}^{n_s+n_t-1}\{|v_{s0\_n}(n)|\} \tag{11}$$

$$\begin{cases} C_p < -V_{set\_p} & \textit{Positive pole} \\ -V_{set\_p} < C_p < V_{set\_p} & \textit{Pole to pole} \\ C_p > V_{set\_p} & \textit{Negative pole} \end{cases} \tag{12}$$

where V_{s0_p} and V_{s0_n} are the GFVTWs of the positive and negative poles at terminal M respectively, and V_{set_p} is the threshold. The calculations are carried out over a data window

of length n_t. V_{set_p} is considered 20kV so that high-resistance internal faults can be reliably detected. In a similar manner, (11) and (12) are used at the receiving terminal as well.

C. Protection Algorithm

The schematic diagram of the proposed protection algorithm is depicted in Fig. 4, which shows the protective process for the sending terminal of the system. Obviously, the protective algorithm at the receiving terminal is very similar.

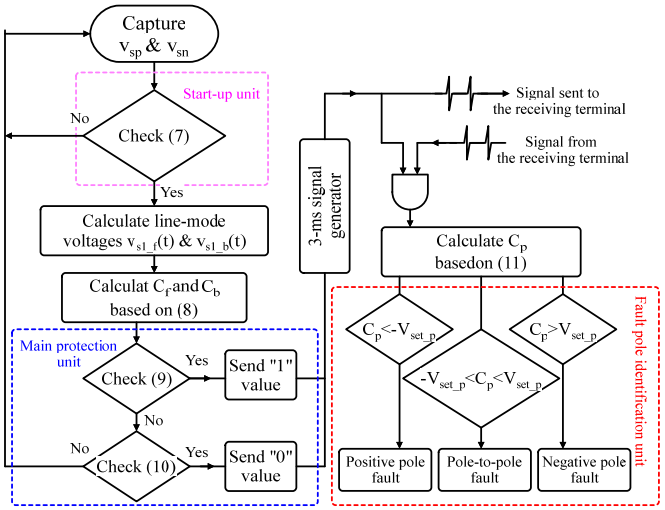

Fig. 4. Schematic diagram of the proposed protection algorithm

The algorithm starts immediately when the start-up unit based on (7) is satisfied. Consequently, V_{s1_f} and V_{s1_b} are calculated and then used to obtain C_f and C_b based on (8). If the main protection thresholds are satisfied according to (9), a 3-ms activation signal with "1" value, as an indication of forward fault, is issued to the protective algorithm at the other terminal. If the protective algorithms receive the activation signals from both terminals within the 3-ms time window, an internal fault situation is confirmed. This means that within the specified 3-ms period, all four LFVTWs and LBVTWs exist at both system terminals and an internal fault has occurred. On the other hand, if (9) is not satisfied, validation of (10) will be checked. If satisfied, a reverse external fault has occurred, thus, a 3-ms prevention signal with "0" value is generated to stop the protective algorithms from issuing a trip signal. If the protective algorithms receives two "1" values from the sending and receiving terminals, they will then initiate the calculation of C_p based on (11). Finally, a trip signal is issued to the corresponding DCCB based on the result of (12).

IV. Simulation Results

The bipolar MMC-HVDC transmission line, illustrated in Fig. 1, is simulated in PSCAD/EMTDC for the performance analysis of the proposed protection method. Various fault scenarios, consisting of internal faults (f_1, f_2 and f_3 in Fig. 1), external faults (f_4 - f_7 in Fig. 1) are considered for the performance analysis. The test system uses the frequency-dependent model of the transmission line and detailed equivalent model of converters with blocking capability [1]. The entire fault scenarios happen at t=50ms, the sampling frequency of the measurement units is 20 kHz and n_t is considered 3 samples. Due to the extensive evaluation of the start-up unit in the literature, performance analysis of this unit will not be further analyzed [6-7].

A. External Faults

The robustness and reliability of the proposed protection method under external faults will be evaluated in detail in this subsection.

Fig. 5 and Fig. 6 show the LFVTWs and LBVTWs generated under external faults at f_4 and f_5 with resistances of 0.1Ω, respectively. According to Fig. 5, it can be seen that immediately after fault initiation, only the forward travelling wave is observed at the sending terminal, which only satisfies (10) at 50.2ms. At this moment, the protective algorithm sends the prevention signal via the communication link to the receiving terminal and the 3-ms decision-making window starts. On the other hand, the initial travelling wave propagates along the transmission line until it reaches the far-end side. Consequently, the protective algorithm of the receiving side is satisfied at 51.2ms based on (9), after which an activation signal is transmitted to the sending terminal. Considering a propagation delay in optical fibers of 200km/ms [23], the prevention signal of the sending side reaches the receiving terminal at 51.7ms, while the activation signal of the receiving terminal reaches the sending terminal at 52.7ms. Since (10) is satisfied at the local terminal and the prevention signal reaches the receiving terminal within the 3-ms time window, none of the protective relays are activated in this case.

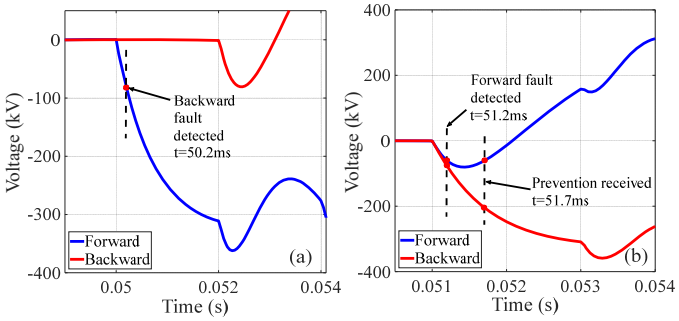

Fig. 5. LFVTWs and LBVTWs at a) sending terminal and b) receiving terminal under the reverse external fault at f_4

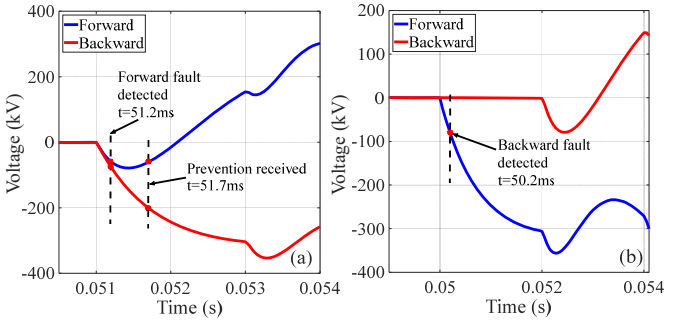

Fig. 6. LFVTWs and LBVTWs at a) sending terminal and b) receiving terminal under the remote-end external fault at f_5

Similar behavior is observed in the case of the remote-end external fault, f_5. As shown in Fig. 6, while only LFVTW is initially detected by the algorithm at the receiving terminal at

50.2ms, both FLVTW and LBVTW are identified at the sending terminal at 51.2ms. However, since the prevention signal is received at 51.7ms at the sending terminal, the protective relays remain inactive under this external fault.

B. Internal Faults

The performance analysis under internal faults is extensively investigated in this study. As examples, a number of these fault cases will be thoroughly discussed here.

Fig. 7 shows the LFVTWs and LBVTWs generated under internal faults at 100km of the positive pole line (f_1 in Fig. 1) with resistance of 1 Ω. Similarly, Fig. 8 shows the results for a PTP fault at 250km with resistance of 500 Ω (f_3 in Fig. 1).

As shown in Fig. 7, the protective algorithm at the sending terminal is able to detect a forward fault at 50.45 with C_f=-237.3kV and C_b=-265.4kV. Likewise, the protective algorithm at the receiving terminal measures C_f=-246.5kV and C_b=-261.9kV and detects a forward fault at 50.8ms. At each detection time, the corresponding algorithm issues the activation signal as an indication of forward fault. The relays at the sending and receiving terminals receive these signals at 52.3 and 51.95ms respectively, and consequently, the fault pole identification units start calculating. Since C_p=-388.8kV and C_p=-308.4kV are obtained at the sending and receiving terminals respectively, the positive pole is correctly identified as the faulty pole.

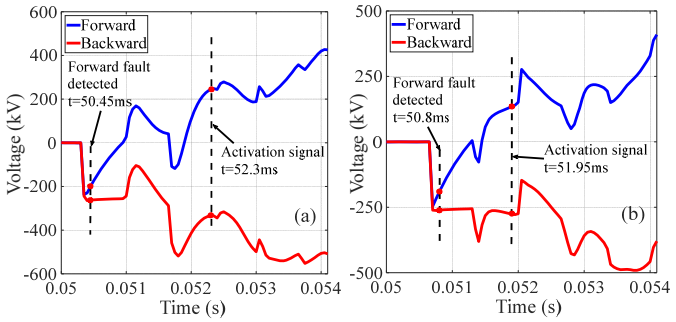

Fig. 7. LFVTWs and LBVTWs at a) sending terminal and b) receiving terminal under the internal PTG fault at 100km

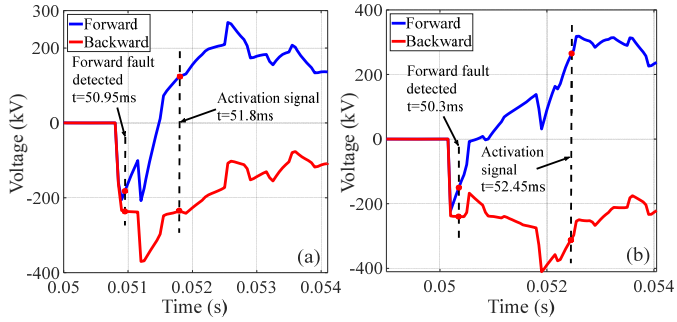

Fig. 8. LFVTWs and LBVTWs at a) sending terminal and b) receiving terminal under the internal PTP fault at 250km

Similarly, under the internal PTP fault at 250km, while the sending terminal algorithm detects a forward fault at 50.95ms with C_f=-205.2kV and C_b=-235.7kV, that at the receiving terminal identifies a forward fault at 50.3ms with C_f=-221.9kV and C_b=-239.1kV. The corresponding activation signals are also received at 51.8 and 52.45ms respectively. Consequently, the fault pole identification unit calculates C_p=0.05kV and C_p=0.04kV at the sending and receiving terminals respectively. Therefore, the trip signal is issued to DCCB of both poles.

C. Sensitivity to Fault Location and Resistance

A robust protective solution should be able to detect internal faults occuring anywhere along the line with various fault resistances. Therefore, performance of the proposed protection method under the variation of fault resistance and location is investigated in this subsection, and a collection of results is gathered in Table 2.

According to Table 2, the measured quantities of C_f and C_b clearly pass their corresponding thresholds at each terminal of the system, hence, the entire fault scenarios are reliably detected by the proposed pilot protection method. Moreover, the faulty poles are also correctly identified at both terminals based on C_p, thus, the protective method is also able to detect the faulty poles reliably.

TABLE II Performance Analysis of Proposed Protection Method in Detecting Internal Faults with Various Fault Locations and Resistances

Fault Data		**Sending terminal measurements (kV)**			**Receiving terminal measurements (kV)**		
Type	***Location/ resistance***	C_f	C_b	C_p	C_f	C_b	C_p
PTG	50 km/1 Ω	-252.4	-270	-428.6	-229.4	-261.6	-224.8
	50km/1000 Ω	-33.5	-38.7	-57.4	-35.6	-38.8	-45.5
	250 km/1 Ω	-227.2	-259.1	-222.6	-249.5	-267.1	-425.1
	250 km/1000 Ω	-33.3	-38.1	-32.6	-36	-38.7	-63.1
NTG	150 km/1 Ω	-238.3	-263.7	369.2	-238.4	-263.6	369
	150 km/1000 Ω	-34.4	-38.3	54.6	-35	-38.6	54.7
PTP	100 km/1 Ω	-603.3	-697	0.03	-635.5	-692.4	-0.08
	100 km/1000 Ω	-125	-144.6	0.05	-131.8	-144	-0.2
	200 km/1 Ω	-632.1	-689.7	0.08	-600.6	-693.8	-0.07
	200 km/1000 Ω	-131.7	-143.4	-0.2	-125	-144	-0.1

Overall, based on the entire simulation study, it can be confirmed that the proposed protection method has high sensitivity, selectivity and reliability in detecting all internal fault scenarios and robust performance in excluding external faults.

D. Comparison to Similar Studies

The main advantages of the proposed pilot protection method are lower computational burden, faster response and higher sensitivity compared to similar studies. For example, the protective criterion presented in [17] uses cosine similarity measure in the protective criterion, while that presented in [18] utilizes Hausdorff distance to detect internal faults. Therefore, both methods have noticeably higher computational burden than the proposed protection method, which is only based on simple derivative functions. Moreover, while a 2-ms data window in required for reliable protection operations in [17] and [18], only 3 samples equal to 150μs is enough for the proposed protection method, which obviously translates into a faster response. As another example, the study presented in [20] uses the arrival time of the fault generated forward and backward current travelling waves to detect internal faults, which is based on the application of wavelet transform and

extraction of modulus maximum at 6th level. Therefore, the computational burden is high. Moreover, the proposed method in [20] needs the time data of the second travelling wave reflections at relays terminals after fault occurrence to operate reliably. This can cause difficulty for the protection as the wave head data of the second reflections can be hard to obtain especially when fault resistance is high. Hence, the proposed protection method, which only relies on the initial travelling waves, has a more robust performance under high resistance faults. Finally, while the protection method in [19] is able to detect internal faults up to 500 Ω, the proposed protection method has higher sensitivity as it is able to provide security under internal faults of up to 1000 Ω, as presented in Table II.

V. Conclusion

A novel pilot protection method based on simultaneous existence of LFVTWs and LBVTWs has been proposed in this paper. It was discussed that under internal faults, both initial FVTW and BVTW waves are observed at each terminal of the system. However, under external faults and based on their direction, one initial FVTW is always missing in one of the terminals. Therefore, a transient-based criterion is designed to check the initial LFVTWs and LBVTWs at each DC terminal to detect internal faults. Moreover, the protective algorithm also utilizes the GFVTW to identify the faulty pole. The protective algorithm issues an activation signal to the other terminal as soon as a forward fault is discovered, or issues a prevention signal if the fault is in reverse direction. The protective algorithm is activated only when a forward fault is detected locally and the activation signal is received from the other terminal. The performance validation of the proposed pilot protection method was conducted using a bipolar HVDC test system, simulated in PSCAD/EMTDC. It was confirmed that the proposed protection method has fast response as only 3 samples equal to $150\mu s$ is enough for reliable operation. Moreover, the proposed method has high sensitivity and selectivity in fault detection for faults occurring anywhere along the line with fault resistances of up to 1000 Ω.

REFERENCES

[1] A. Gandomkar, A. Parastar, and J. K. Seok, "High-power multilevel step-up DC/DC converter for offshore wind energy systems," *IEEE Trans. Ind. Electron.*, vol. 63, pp. 7574-7585, 2016

[2] P. Mitra, L. Zhang, and L. Harnefors, "Offshore wind integration to a weak grid by VSC-HVDC links using power-synchronization control: A case study," *IEEE Trans. Power Del.*, vol. 29, pp. 453-461, 2014

[3] F. D. Marvasti, and A. Mirzaei. "A novel method of combined DC and harmonic overcurrent protection for rectifier converters of Monopolar HVDC systems," *IEEE Trans on Power Del,* vol. 33, no. 2, pp. 892-900, 2018.

[4] O. G. Bellmunt, A. J. Ferre, A. Sumper, and J. B. Jane, "Control of a wind farm based on synchronous generators with a central HVDC-VSC converter," IEEE Trans. Power Syst., vol. 26, no. 3, pp. 1632–1640, Aug. 2011.

[5] Y. Ge, L. Xiang, Y. Li, R. He and W. Liu, "A novel topology for HVDC link connecting to offshore wind farms," *2020 IEEE International Conference on High Voltage Engineering and Application (ICHVE)*, 2020, pp. 1-4

[6] X. Zheng, M. H. Nadeem, N. Tai, S. Habib, B. Wang, M. Yu, and Y. He, "A transient current protection and fault location scheme for MMC-HVDC transmission network," *Int J Electr Power Energy Syst*, vol. 124, 2021

[7] Z. Xiaodong, T. Nengling, Z. Wu, and S. T. James, "Harmonic current protection scheme for voltage source converter-based high-voltage direct current transmission system," *IET Gen Transm Distrib,* vol. 8, no. 9, pp. 1509–1515, 2014

[8] Z. Chen, G. Song, Z. Liang, W. Li and Z. Fan, "A pilot protection principle for MMC-HVDC transmission lines based on charge balance," *2019 IEEE 8th International Conference on Advanced Power System Automation and Protection (APAP)*, 2019, pp. 303-306

[9] J. Sneath, and A. D. Rajapakse, "Fault detection and interruption in an earthed HVDC grid using ROCOV and hybrid DC breakers," *IEEE Trans Power Del*., vol.31, no.3, pp:973–981, 2016

[10] W. Leterme, J. Beerten, and D. Van Hertem, "Nonunit protection of HVDC grids with inductive DC cable termination," *IEEE Trans Power Del.,* vol.31, no.2, pp:820–828, 2016

[11] J. Zheng, M. Wen, Y. Chen and X. Shao, "A novel differential protection scheme for HVDC transmission lines," *Int J Electr Power Energy Syst,* vol. 94, pp. 171-178, 2018

[12] M. Gamal Muhammad, D. Mourad Hafez, and A. Mahmoud Abd-Elaziz, "Novel HVDC transmission line protection scheme based on current differential," 2018 Twentieth International Middle East Power Systems Conference (MEPCON), 2018, pp. 361-366

[13] X. Chu, "Unbalanced current analysis and novel differential protection for HVDC transmission line based on the distributed parameter model," *Electric Power Sys. Res.,* vol.171, pp:105-115, 2019

[14] Z. Dai, N. Liu, C. Zhang, X. Pan, and J. Wang, "A pilot protection for HVDC transmission lines based on transient energy ratio of DC filter link," *IEEE Trans. Power Del.,* vol. 35, no. 4, pp:1695-1706, 2020

[15] Y. Zang, Y. Li, J. Song, B. Li, and X. Chen, "A new protection scheme for HVDC transmission lines based on the specific frequency current of DC filter," *IEEE Trans Power Del.,* vol. 34, no. 2, pp. 420-429, 2019

[16] F. D. Marvasti, A. Mirzaei, M. E. H. Golshan, "Novel pilot protection scheme for line-commutated converter high voltage direct current transmission lines based on behaviour of characteristic harmonic impedances," *IET Gener Transm Distrib*.,vol. 15, no. 2, pp: 264-278, 2020

[17] Y. Wang, Z. Hao, B. Zhang and F. Kong, "A pilot protection scheme for transmission lines in VSC-HVDC grid based on similarity measure of traveling waves," *IEEE Access*, vol. 7, pp. 7147-7158, 2019

[18] Q. Huai, L. Qin, K. Liu, A. Hooshyar, H. Ding, C. Gong, and Y. Xu, "A pilot line protection for MT-HVDC grids using similarity of traveling waveforms," *Int J Electr Power Energy Syst*, vol. 131, 2021

[19] H. Cao, M. Xie, Z. Zhou, X. Wang, B. Yu, D. Du,H. Wang, T. Wang and Y. Yu, "A pilot protection scheme for UHVDC lines based on backward traveling-wave difference," *2019 IEEE 8th International Conference on Advanced Power System Automation and Protection (APAP)*, 2019, pp. 85-90

[20] L. Jiang, Q. Chen, W. Huang, Y. Zeng, L. Wang, and P. Zhao, "A novel directional pilot protection method for VSC-MTDC based on the initial forward and backward travelling wave head," *Int J Electr Power Energy Syst*, vol. 109, pp. 198-206, 2019

[21] L. Xiaopeng, T. Yong, and T. Yufei, "A pilot protection method based on amplitude comparison of backward traveling wave for HVDC transmission lines," *Power System Technology*, vol.40, no.10, pp. 3095-3101, 2016

[22] Y. Zhang, N. Tai and B. Xu, "Fault analysis and traveling-wave protection scheme for bipolar HVDC lines," *IEEE Trans. Power Del.*, vol. 27, no. 3, pp. 1583-1591, 2012

[23] B. Li, M. Lv, B. Li, S. Xue, and W. Wen, "Research on an improved protection principle based on differential voltage traveling wave for VSC-HVDC transmission lines," *IEEE Trans. Power Del.*, vol. 35, no. 5, pp. 2319-2328, 2020